A Novel Analysis of Microstrip Structures Using the Gaussian Green's Function Method

Mohammad Mahdi Tajdini, *Student Member, IEEE*, and Amir Ahmad Shishegar, *Member, IEEE*

***Abstract*—A novel closed form expression is derived for spatial Green's functions of microstrip structures by expanding the spectral Green's function into a Gaussian series. This innovative method is called the Gaussian Green's function (GGF) method due to the Gaussian form in the closed form Green's function representation. The main advantage of the GGF method lies in its precision as well as rapid convergence. To demonstrate the versatility of this method, the current distribution of a microstrip antenna is achieved via the combination of the method of moments (MoM) and GGF method. It is shown that this method can be computationally very efficient with less than 1% error compared to the numerical integration of the spectral integral. Also, the results of the GGF method have been compared to the results of the commercial full-wave software of Agilent ADS.**

***Index Terms*—Gaussian Green's function method, Green's function, microstrip structure.**

I. Introduction

MICROSTRIP structures are widely utilized in printed antennas, monolithic microwave integrated circuits (MMIC's), and high speed digital circuits. Microwave components such as filters, couplers, and power dividers can be manufactured easily by the microstrip technology while they are extremely cheaper, lighter, and more compact than traditional waveguide structures [1]. For instance, the excellent conformability of microstrip antennas and their low cost have made them exceptionally ideal for wireless local area network (WLAN) applications [2].

In the modeling and analysis of microstrip structures especially on a large scale like printed antenna arrays, whereas the full-wave methods are not useful, the method of moments (MoM) [3] is commonly used owing to its efficiency, accuracy and applicability to various structures [4]–[6]. This method can be employed successfully to solve the mixed potential integral equation (MPIE). The important advantage of the MPIE lies in its weakly singular kernel [7]. The solution of this equation in the spatial domain usually entails the acquaintance of the spatial Green's function. For layered media, the major problem of the approach is that the matrix approximant to the MPIE requires repetitive evaluation of the spatial Green's function. To find this function, much attempt should be devoted to the calculation of Sommerfeld integrals, whose integrand is composed of the closed form spectral Green's function and the Hankel or exponential function as the kernel. This type of representation of the Green's function is time-consuming and very expensive [8]. Therefore, the numerical appraisal of the system matrix is computationally inefficient.

There are various kinds of method to make the computation of the matrix elements more efficient. One of the common approaches is based on the approximation of the spectral Green's function by a finite series of properly chosen terms that can be transformed into the spatial domain leading to a closed form representation of the function. The image method is available for microstrip structures, although it is still time-consuming to some extent [9]. The complex images (CI) method approximates the spatial Green's function utilizing a finite number of images of an infinitesimal source radiating in a homogenous unbounded area. The amplitudes and locations of these images can be complex values [10]–[12]. This semi-analytical method approximates the spectral Green's function by a series of complex exponential functions. This can be acquired by any appropriate method like the simple Prony method, the least square Prony method or the generalized pencil of functions (GPOF) method [13], [14]. Then, the spectral Green's function can be transformed to the spatial domain utilizing the Sommerfeld identity [8], resulting in a closed form spatial Green's function. Nevertheless, there are some substantial difficulties in actual implementation of the method. For instance, the CI method has no built-in convergence measure and its precision can merely be determined a periori by testing the results with those achieved by the numerical integration of the Sommerfeld integral [15]. Moreover, the critical convergence takes place in some cases of the CI method when the Prony method is used. In other words, the accuracy of the approximation of the Green's function is sensitive to the number of images and utilizing many complex images sometimes leads to divergence of the results [11], although this problem has been solved in the newer versions of the CI method [16]. There are other difficulties in the CI method which have been pointed out in the literature [10], [17]. Another method is the steepest descent path (SDP) method which has been exploited in the calculation of the layered media Green's functions [18]. However, this method is applicable in far field problems, e.g., in the case of scattering in large distances from the source.

One of the well-known mathematical functions is the Gaussian function. This function identifies the significant electromagnetic radiation called the Gaussian beam whose electric field and intensity (irradiance) profiles are associated with the Gaussian function [19]. The Gaussian beam is a solution of the paraxial Helmholtz equation. It is also a very

Manuscript received August 30, 2008; revised May 20, 2009. First published November 06, 2009; current version published January 04, 2010.

M. M. Tajdini was with Sharif University of Technology, Tehran 11365-8639, Iran. He is now with the Department of Electrical and Computer Engineering, Northeastern University, Boston, MA 02115 USA (e-mail: mtajdini@ece.neu.edu).

A. A. Shishegar is with the Department of Electrical Engineering, Sharif University of Technology, Tehran 11365-8639, Iran (e-mail: shishegar@ee.sharif.edu).

Digital Object Identifier 10.1109/TAP.2009.2036191

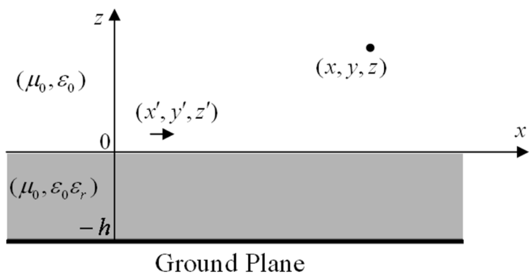

Fig. 1. An infinitesimal horizontal electric dipole above an open microstrip substrate.

good approximation for many laser outputs. It is important to know that the Hankel transform of the Gaussian function is another Gaussian function. Therefore, the Gaussian function is a self-dual function [20]. In other words, this function is an eigenfunction of the Hankel transform operator. These facts are used to develop a more physical alternative to the CI method.

In this paper, a new closed form representation for the spatial Green's function of the microstrip structure is introduced. It is accomplished by expanding the spectral Green's function into a series of Gaussian functions and making the inverse Hankel transformation to obtain the spatial Green's function in another Gaussian series. The method is called the Gaussian Green's function (GGF) method owing to the Gaussian form in the new closed form Green's function representation [21]. The main advantage of the GGF method lies in its precision as well as rapid convergence. If the multilayer media Green's functions are achieved in closed form as a summation of a few Gaussian functions, the MoM matrix entries can be calculated easily in the analytical form leading to a significant decrease in the matrix filling time. The result of this method can be valid over a range of distances, i.e., from nearly $1.5 \times 10^{-4}\lambda$ to 1.5λ. The parameters of the Gaussian terms required for the expansion of the Green's function can be chosen in conformity with some simple criteria. Exploiting methods like the Gabor expansion method [22], the point matching method, or the minimum least squares method for expanding the spectral Green's function into a Gaussian series, one can have an approximation method with the built-in convergence measure [23], [24]. Furthermore, the critical convergence does not appear in the GGF method because the precision of the Green's function approximation in this method is not as sensitive to the number of series terms as it is in the CI-Prony method.

This paper is organized as follows. In Section II, the Green's function of an open microstrip structure is considered and the CI method is briefly explained. Section III elucidates the theory of the GGF method and derives the simple closed form expression to find the Green's function of the open microstrip structure. The effect of the surface waves and the expansion methods are also considered in this section. To evaluate the accuracy and performance of this method, the GGF method in conjunction with the MoM is employed in Section IV to acquire the current distribution of a microstrip antenna as a practical example of microstrip structures. Numerical results are given in this section and the GGF method is compared to the numerical integration of the spectral integral. Eventually, conclusion is provided in Section V.

II. The Green's Function of an Open Microstrip Structure

For some electromagnetic problems including microstrip structures, the Green's function can be found analytically in a closed form in the spectral domain and the dyadic and scalar spatial Green's function $G_A^{\rm xx}$ and G_q [15], [25] can be specified using the Sommerfeld integral in the following form [8]:

$$G_A^{\rm xx}(\rho, z) = \frac{1}{4\pi}\int_{-\infty}^{+\infty} \tilde{G}_A^{xx}(k_\rho, z) H_0^{(2)}(k_\rho \rho) k_\rho dk_\rho \quad (1a)$$

$$G_q(\rho, z) = \frac{1}{4\pi}\int_{-\infty}^{+\infty} \tilde{G}_q(k_\rho, z) H_0^{(2)}(k_\rho \rho) k_\rho dk_\rho \quad (1b)$$

$$\rho = \sqrt{(x-x')^2 + (y-y')^2}. \quad (1c)$$

In (1), $H_0^{(2)}(\cdot)$ is the second kind Hankel function of zero order, $\tilde{G}_A^{xx}$ stands for the x-component of spectral vector potential created due to an infinitesimal x-directed electric dipole, and by the same token $\tilde{G}_q$ stands for the spectral scalar potential created owing to one charge of the dipole.

For an infinitesimal horizontal electric dipole located above an open microstrip substrate, as shown in Fig. 1, these spectral potentials in the air region can be given by [26]

$$\tilde{G}_A^{xx} = \frac{\mu_0}{j2\beta_{z0}}[\exp(-j\beta_{z0}(z-z')) + R_A \exp(-j\beta_{z0}(z+z'))] \quad (2a)$$

$$\tilde{G}_q = \frac{1}{j2\varepsilon_0\beta_{z0}}[\exp(-j\beta_{z0}(z-z')) + (R_A + R_q)\exp(-j\beta_{z0}(z+z'))] \quad (2b)$$

where

$$R_A = -\frac{r_{10}^{TE} + \exp(-j2\beta_{z1}h)}{1 + r_{10}^{TE}\exp(-j2\beta_{z1}h)} \quad (3a)$$

$$R_q = -\frac{2\beta_{z0}^2(1-\varepsilon_r)(1-\exp(-j4\beta_{z1}h))}{(\beta_{z1}+\beta_{z0})(\beta_{z1}+\varepsilon_r\beta_{z0})S} \quad (3b)$$

$$S = \left(1 + r_{10}^{TE}\exp(-j2\beta_{z1}h)\right) \times \left(1 - r_{10}^{TM}\exp(-j2\beta_{z1}h)\right) \quad (3c)$$

R_A and R_q indicate the effect of the open microstrip substrate where r_{10}^{TE} and r_{10}^{TM} are defined as

$$r_{10}^{TE} = \frac{\beta_{z1} - \beta_{z0}}{\beta_{z1} + \beta_{z0}}, \quad r_{10}^{TM} = \frac{\beta_{z1} - \varepsilon_r\beta_{z0}}{\beta_{z1} + \varepsilon_r\beta_{z0}} \quad (4a)$$

$$\beta_{z0} = \sqrt{k_0^2 - k_\rho^2}, \quad \beta_{z1} = \sqrt{\varepsilon_r k_0^2 - k_\rho^2} \quad (4b)$$

where k_0 is the wave number in the air region and β_{z0} and β_{z1} are the propagation constants along the z -direction in the air and substrate, respectively.

The Sommerfeld integral as shown in (1) can not be calculated analytically in general, except a few special cases. There are a great number of articles in the literature covering a very broad range of numerical methods that have been proposed so far to overcome this problem [15], [27]. For example, a successive semi-analytical method is the CI method. To apply the CI method, a proper exponential function expansion is done in the spectral domain [11]. This can be acquired by any appropriate method like the simple Prony method, the least square Prony method or the generalized pencil of functions (GPOF) method [13], [14]. Then, the spectral Green's function is transformed to the spatial domain using the Sommerfeld identity [8], resulting in a closed form spatial Green's function of complex images. In other words, the total spatial Green's function is represented in a finite series of images of an infinitesimal source radiating in a homogenous unbounded area, when both the amplitudes and locations of these images can be complex values [12]. This method has limitations which have been pointed out extensively in the literature [10], [15], [17].

III. The Gaussian Green's Function Method

A typical Gaussian function can be described as

$$g(\rho) = A_0 \exp(-\alpha_0 \rho^2) \tag{5}$$

where A_0 represents the Gaussian function's maximum and α_0 is the constant which represents the spreading of the Gaussian function. It can be shown that for the Gaussian function, the inverse Hankel transform relation is [20]

$$\exp(-\alpha_0\rho^2) = \frac{1}{4\pi}\int_{-\infty}^{+\infty} \frac{\pi}{\alpha_0} \exp\left(-\frac{k_\rho^2}{4\alpha_0}\right) H_0^{(2)}(k_\rho \rho) k_\rho dk_\rho. \tag{6}$$

It means that the Gaussian function is a self-dual function, i.e., the Hankel transform of the Gaussian function is another Gaussian function. Thus, the Gaussian function is an eigenfunction of the Hankel transform operator.

The Gaussian Green's function (GGF) method is derived through the expansion of the spectral Green's function into a Gaussian series as an alternative to the exponential series in the CI method. Consider the dyadic and scalar spectral Green's functions $\tilde{G}_A^{xx}$ and $\tilde{G}_q$ of (2) for example. After extracting the source terms, they are expanded into series of Gaussian terms, i.e.,

$$\tilde{G}_{A0}^{xx} \cong \sum_{m=1}^{M} \frac{\pi A_m}{\alpha_m} \exp\left(-\frac{k_\rho^2}{4\alpha_m}\right) \tag{7a}$$

$$\tilde{G}_{q0} \cong \sum_{n=1}^{N} \frac{\pi A'_n}{\alpha'_n} \exp\left(-\frac{k_\rho^2}{4\alpha'_n}\right) \tag{7b}$$

when

$$\tilde{G}_{A0}^{xx} = \tilde{G}_A^{xx} - \frac{\mu_0}{j2\beta_{z0}} \exp(-j\beta_{z0}(z-z')) \tag{8a}$$

$$\tilde{G}_{q0} = \tilde{G}_q - \frac{1}{j2\varepsilon_0\beta_{z0}} \exp(-j\beta_{z0}(z-z')). \tag{8b}$$

Making the inverse Hankel transformation to the spectral Green's functions and using (6), then we can attain the dyadic and scalar spatial Green's functions G_A^{xx} and G_q by another series of Gaussian functions, i.e.,

$$G_A^{xx} \cong \frac{\mu_0}{4\pi r_0} \exp(-jk_0 r_0) + \sum_{m=1}^{M} A_m \exp(-\alpha_m \rho^2) \tag{9a}$$

$$G_q \cong \frac{1}{4\pi\varepsilon_0 r_0} \exp(-jk_0 r_0) + \sum_{n=1}^{N} A'_n \exp(-\alpha'_n \rho^2) \tag{9b}$$

$$r_0 = \sqrt{\rho^2 + (z-z')^2} \tag{9c}$$

where the Sommerfeld identity [8] has been applied for the first exponential term. These closed form expressions are the results of applying the Gaussian Green's function (GGF) method [21]. It is noted that the GGF method is based on the expansion of the spectral Green's function into a Gaussian series. The coefficients of (7) can be found exploiting the Gabor expansion method [22]. One advantage of the Gabor expansion method is that in this method, completeness is a posteriori. It also removes any arbitrariness in the preference of coefficients once the number of Gaussian terms is selected. Nevertheless, in this method finding the coefficients of the Gaussian series in (7) generally necessitates a moderately intricate numerical computation of biorthogonal integrals [23]. The coefficients of Gaussian series can be found in simpler and more straightforward approach using the point matching method or the minimum least squares method [24]. Thus, the relation between (2) and (7) can be reduced to a set of linear equations which can be solved simultaneously utilizing matrix inversion. The choice of the Gaussian expansion parameters can be carried out according to some simple criteria. For example, the number of Gaussian terms may be taken in the range of 7–9 to achieve the accuracy of 1%. The alpha parameters in (7) can be chosen to obtain the least squares error. In practice, the simple point matching method can be performed and the coefficients can be adjusted by trial and error to obtain best results. The coefficients of the Gaussian series in (7) are dependent on the source and field locations z and z'. However, in many problems including the calculation of the current distribution of the microstrip antenna considered in the succeeding section of this paper, the z and z' are fixed relative to each other. Thus, only one expansion is necessary to approximate the spatial Green's function. The z-independent formulation of the GGF method is currently under study.

The inverse Hankel transform can be carried out along the real axis C_r on the complex k_ρ plane as shown in Fig. 2(a). The equivalent contour of C_r on the complex β_{z0} plane $(-j\infty \to 0 \to k_0 \to 0 \to -j\infty)$ is demonstrated in Fig. 2(b). We can approximate this contour by an oblique line, C_d, illustrated in Fig. 2(b). It is noticed that the truncation point of the approximation path, $-jk_0T_0$, should be sufficiently selected near to or far from the origin of the complex β_{z0} plane to afford adequate information from the spectral Green's function for the far field or near field approximation respectively. The corresponding contour of C_d on the complex k_ρ plane is demonstrated in Fig. 2(a) which is along a deformed integration contour passing through the origin and lying in the first and third quadrants of coordinates. Any deformed integration contour can be used while no more singularity is encountered in the deformation. Owing to the notable resemblances between the CI and GGF methods, for

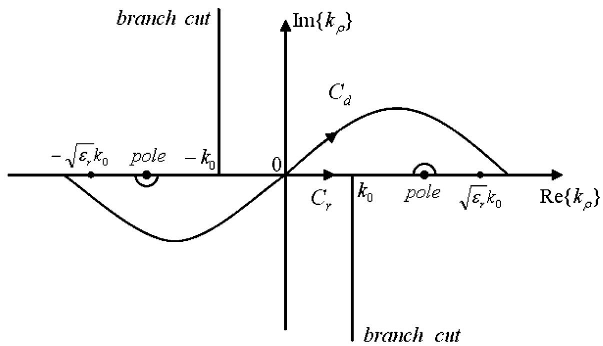

(a)

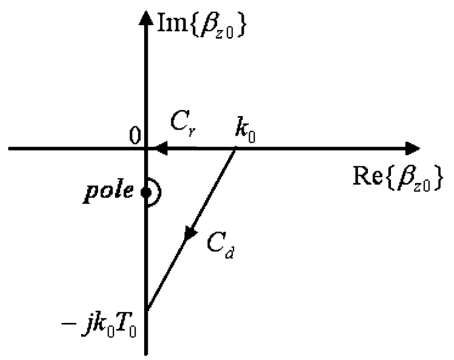

(b)

Fig. 2. The integration contours C_r and C_d: (a) on the complex k_ρ plane and (b) on the complex β_{z0} plane.

improvement of the approximation especially in large distances, some useful techniques such as modification of the integration contour or extraction of the surface wave poles can be examined [26].

$\tilde{G}_A^{xx}$ and $\tilde{G}_q$ can have poles on the real axis of the complex k_ρ plane. These poles are attributed to the source of propagating surface waves. The poles in $[-k_0, k_0]$ stand for the surface waves trapped by the bottom ground plane and the poles in $[-\sqrt{\varepsilon_r}k_0, -k_0]$ or $[k_0, \sqrt{\varepsilon_r}k_0]$ epitomize the surface waves trapped by the dielectric slab [11]. The effect of surface waves is usually dominant in the far field region and may constitute a major problem for accuracy of methods based on the Hankel transform such as the CI or GGF method in large distances. To overcome this problem, all the surface wave poles can be extracted from the spectral Green's function and the spatial Green's function can be signified as a summation of two series. To be more explicit, by extracting all the surface wave poles from the dyadic and scalar spectral Green's functions, the results can be expanded into series of Gaussian functions, i.e.,

$$\tilde{G}_{A0}^{xx} - \sum_{p=1}^{P} \frac{2k_{\rho p}R_p}{k_\rho^2 - k_{\rho p}^2} \cong \sum_{m=1}^{M} \frac{\pi A_m}{\alpha_m} \exp\left(-\frac{k_\rho^2}{4\alpha_m}\right) \quad (10a)$$

$$\tilde{G}_{q0} - \sum_{q=1}^{Q} \frac{2k'_{\rho q}R'_q}{k_\rho^2 - k'^2_{\rho q}} \cong \sum_{n=1}^{N} \frac{\pi A'_n}{\alpha'_n} \exp\left(-\frac{k_\rho^2}{4\alpha'_n}\right) \quad (10b)$$

where $k_{\rho p}$ and R_p are the pth surface wave pole and the residue of $\tilde{G}_A^{xx}$ at this pole, respectively. Also, $k'_{\rho q}$ and R'_q are the q th surface wave pole and the residue of $\tilde{G}_q$ at this pole, respectively. R_p and R'_q are given by [26]

$$R_p = \lim_{k_\rho \to k_{\rho p}} (k_\rho - k_{\rho p})\tilde{G}_{A0}^{xx},$$
$$R'_q = \lim_{k_\rho \to k'_{\rho q}} (k_\rho - k'_{\rho q})\tilde{G}_{q0}. \quad (11)$$

According to the Cauchy's integral formula [28]

$$\frac{1}{j2\pi} \oint \frac{f(z)}{z - z_0} dz = f(z_0). \quad (12)$$

Substituting (10) in (1) and utilizing (6) and (12), we can have the closed form dyadic and scalar spatial Green's functions as

$$G_A^{xx} \cong \frac{\mu_0}{4\pi r_0}\exp(-jk_0r_0) + \sum_{m=1}^{M} A_m \exp(-\alpha_m\rho^2) - \frac{j}{2}\sum_{p=1}^{P} R_p H_0^{(2)}(k_{\rho p}\rho)k_{\rho p} \quad (13a)$$

$$G_q \cong \frac{1}{4\pi\varepsilon_0 r_0}\exp(-jk_0r_0) + \sum_{n=1}^{N} A'_n \exp(-\alpha'_n\rho^2) - \frac{j}{2}\sum_{q=1}^{Q} R'_q H_0^{(2)}(k'_{\rho q}\rho)k'_{\rho q}. \quad (13b)$$

Thus, the closed form spatial Green's function can be represented as the contribution of a spherical wave, a finite number of Gaussian beams, and a finite number of cylindrical waves. The surface wave expressions have been taken in [11] and [26] as a constitutive part of the approximation in all distances from the source. Nevertheless, we consider them here as a far field approximation on the air-dielectric interface. It is noticed that non-real poles that represent the surface waves in a lossy medium are not extracted since they are damped and disappeared at far distances. Thus, their contribution can be incorporated in the Gaussian series. There are other sources of deterioration of the approximation for large distances, such as artificial branch cuts. However, as it has been demonstrated in [8] and [29], the contribution of non-physical branch points to the spatial Green's function can not be the main source of the problem in the far field approximation. The reason is that the branch cut contribution is asymptotically as $1/\rho^2$ at the interfaces, while the surface wave contribution is as $1/\sqrt{\rho}$. Therefore, the branch cut contribution decays faster than the surface wave contribution and can be involved in the Gaussian series of (13).

IV. Numerical Results

In this section, a number of numerical examples are presented to show the efficiency and versatility of the GGF method. At first, the microstrip antenna of Fig. 3 as a simple but intuitive example is considered to display the accuracy of the GGF method. This patch antenna consists of a rectangular conducting strip separated from an infinite ground plane by a relatively thick substrate and is fed at the mid point of the metallization strip. The relative permittivity of the substrate $\varepsilon_r = 4.3$, the substrate

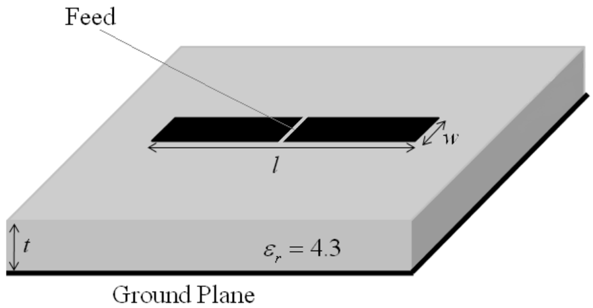

Fig. 3. A planar microstrip antenna on an infinite ground plane.

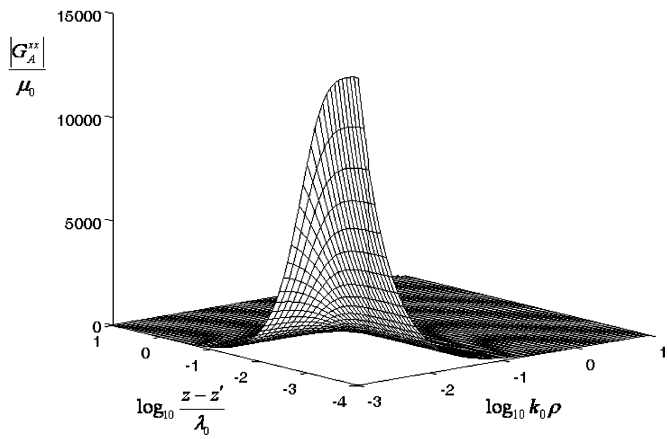

Fig. 4. The amplitude of G_A^{xx}/μ_0 for the open microstrip structure of Fig. 1 when $z' = 0$, $h = 0.8\lambda_0$, and $\varepsilon_r = 4.3$.

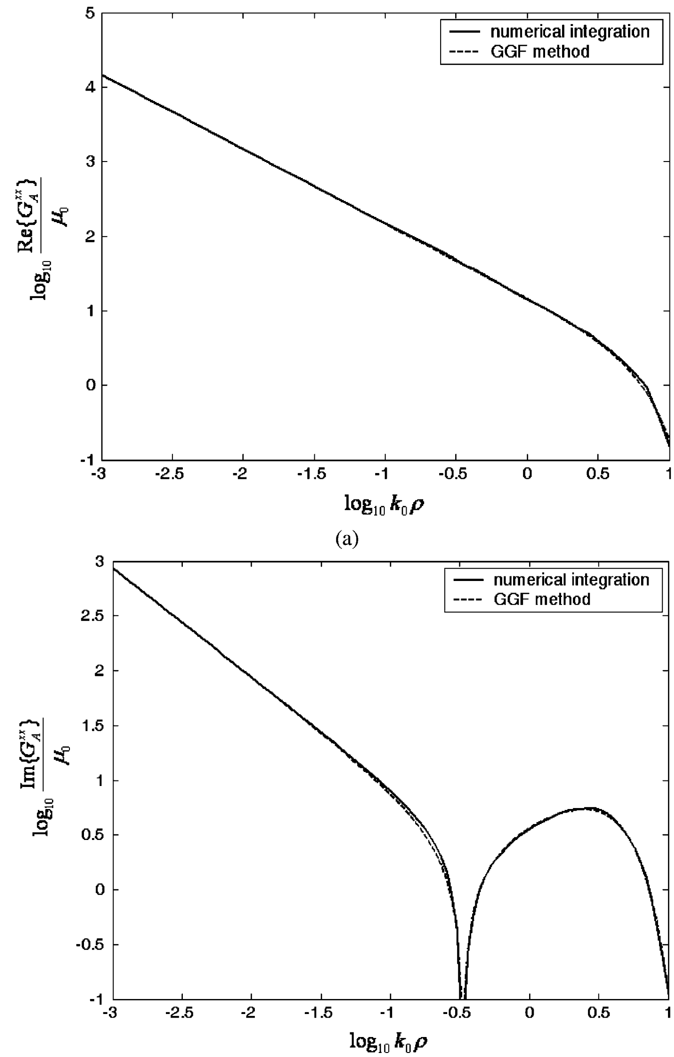

(b)

Fig. 5. Comparison of the GGF method with the numerical integration: (a) real and (b) imaginary parts of G_A^{xx}/μ_0 for the open microstrip structure of Fig. 1 when $z = z' = 0$, $h = 0.8\lambda_0$, and $\varepsilon_r = 4.3$.

thickness $t = 5$ cm, the strip length $l = 1.7$ cm, the strip width $w = 0.08$ cm, the characteristic impedance of the coaxial cable $Z_0 = 50\ \Omega$, and the frequency $f = 4.8$ GHz.

The analysis of this structure is customarily performed using the MoM. This usually requires the acquaintance of the spatial Green's function of the structure. Therefore, the computation of the spatial Green's function of the open microstrip structure, as shown in Fig. 1, looks inevitable. In this case, an infinitesimal horizontal electric dipole is located at $z' = 0$ while $h = 0.8\lambda_0$ and $\varepsilon_r = 4.3$. For the sake of brevity, solely G_A^{xx} is demonstrated. Fig. 4 roughly shows the dyadic Green's function G_A^{xx} as a function of ρ and z. In Fig. 5, this function is approximated by the GGF method and compared with the results of the numerical integration where $z = z'$. Comparison of the 7-term closed form Green's function achieved through the GGF method with the numerical integration makes obvious that the difference between these two results can be unobservable with less than 1% error when compared to the numerical integration. The codes for the numerical integration and the GGF method have been carried out on a 3.2 GHz personal computer. It is perceived that the CPU time recorded for the approximation of the Green's function utilizing the GGF method can be more than 20 times faster than the numerical integration.

Fig. 6 demonstrates the current distribution of the microstrip antenna of Fig. 3 computed by the combination of the MoM and GGF method which can agree well with the implementation of the MoM through the numerical integration of the spectral integral. According to the numerical integration of the spectral integral in conjunction with the MoM, the input impedance of the antenna can be achieved about $Z_{\rm in} = 51 - j2\ \Omega$ (VSWR $= 1.046$). By combination of the MoM and GGF method, the method that is presented in this paper, the input impedance can be accomplished as $Z_{\rm in} = 50.5 - j2.1\ \Omega$ (VSWR $= 1.043$) that can be in good agreement. Moreover, the antenna of Fig. 3 has been analyzed by the commercial software of Agilent ADS [30] and the current distribution of the antenna has been compared to the results of the GGF method. The input impedance of the antenna can be obtained about $Z_{\rm in} = 52 + j0\ \Omega$ (VSWR $= 1.040$). The simulation results are also plotted in Fig. 6.

As a final remark, the microstrip structure of Fig. 1 is considered to demonstrate the validity of the GGF method in a variety of frequencies, thicknesses and permittivities. Thus, at the frequencies of $f = 2.4$ GHz, $f = 4.8$ GHz, and $f = 9.6$ GHz the amplitude of the dyadic Green's function is acquired via

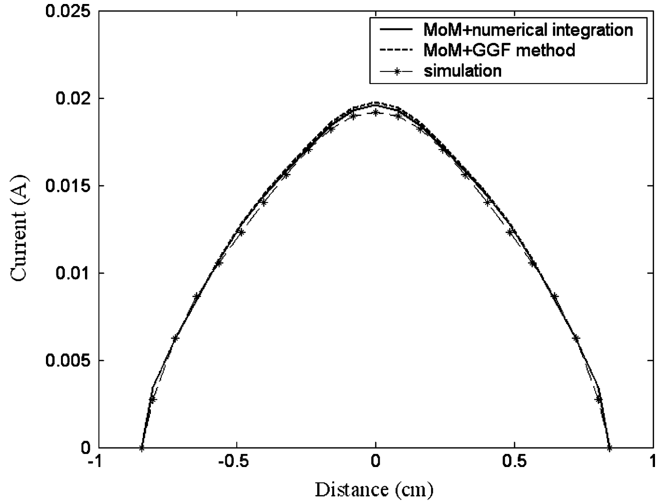

Fig. 6. The current distribution on the horizontal axis of the microstrip antenna of Fig. 3 when $l = 1.7$ cm, $w = 0.08$ cm, $t = 5$ cm, $\varepsilon_r = 4.3$, and $f = 4.8$ GHz obtained from the MoM via the GGF method, MoM via the numerical integration and the simulation results.

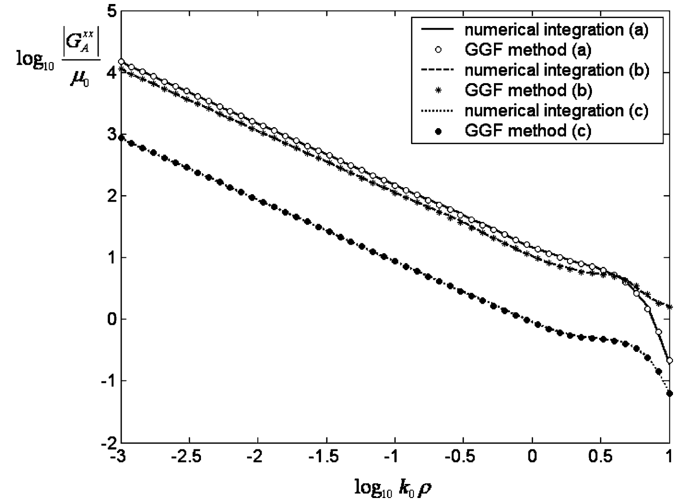

Fig. 8. Comparison of the GGF method with the numerical integration: The amplitude of $G_A^{xx}\mu_0$ for the open microstrip structure of Fig. 1 when $z = z' = 0$ and $f = 4.8$ GHz for: (a) $h = 5$ cm, $\varepsilon_r = 4.3$, (b) $h = 14$ cm, $\varepsilon_r = 4.3$, and (c) $h = 14$ cm, $\varepsilon_r = 8.3$.

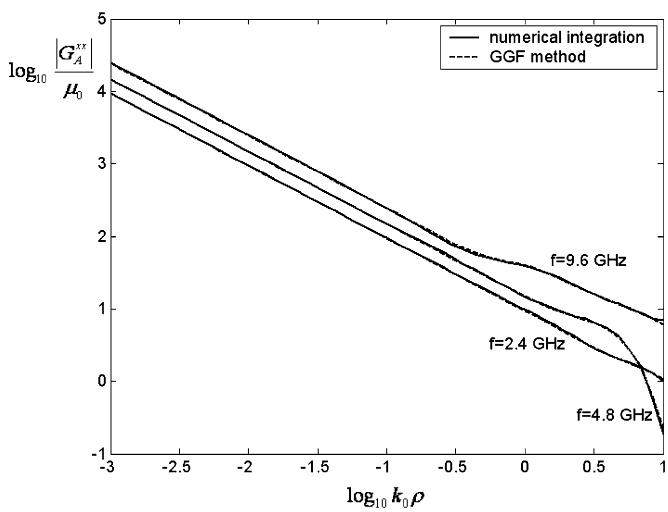

Fig. 7. Comparison of the GGF method with the numerical integration: The amplitude of $G_A^{xx}\mu_0$ for the open microstrip structure of Fig. 1 when $z = z' = 0$, $h = 5$ cm, and $\varepsilon_r = 4.3$ at $f = 2.4$ GHz, $f = 4.8$ GHz, and $f = 9.6$ GHz.

the GGF method and illustrated in Fig. 7 which can be in good agreement with the results of the numerical integration where $z = z' = 0, h = 5$ cm, and $\varepsilon_r = 4.3$. Then, this microstrip structure is considered in the frequency of $f = 4.8$ GHz but when the thickness of the substrate has been changed to $h = 14$ cm and also when the permittivity of the substrate has been altered to $\varepsilon_r = 8.3$. The results of the GGF method are compared to the numerical integration in Fig. 8 which can be in good agreement for all these cases.

V. Conclusion

The spectral integral solution for the calculation of spatial Green's functions of microstrip structures is typically time-consuming and computationally inefficient. This paper introduces an innovative method to derive a closed form expression for the Green's function by expanding the spectral Green's function into a series of Gaussian terms. With this method, the numerical integration of the spectral integrals can be avoided entirely, leading to a considerable decrease of calculating time. The comparison of the GGF method with the numerical integration indicates the precision and efficiency of this method. Furthermore, the combination of the MoM and GGF method is suggested as an efficient and versatile method for analysis of microstrip structures. Even though only a printed antenna with one substrate layer is studied, the method of this paper can be correspondingly applied to the multilayered microstrip structures.

Acknowledgment

The authors would like to earnestly thank the reviewers for their constructive comments.

References

[1] Y. S. Tan, X. S. Rao, L. F. Chen, C. Y. Tan, and C. K. Ong, "Simulation, fabrication and testing of a left-handed microstrip coupler," *Microw. Opt. Technol. Lett.*, vol. 45, no. 3, pp. 255–258, May 2005.

[2] M. M. Tajdini and M. Shahabadi, "Wideband planar log-periodic antenna," in *Proc. IEEE Int. Workshop Antenna Technol.*, Mar. 21–23, 2007, pp. 331–334.

[3] R. F. Harrington, *Field Computation by Moment Methods*. New York: Wiley-IEEE Press, 1993.

[4] T. Onal, M. I. Aksun, and N. Kinayman, "A rigorous and efficient analysis of 3-D printed circuits: Vertical conductors arbitrarily distributed in multilayer environment," *IEEE Trans. Antennas Propag.*, vol. 55, no. 12, pp. 3726–3729, Apr. 2006.

[5] S. N. Makarov, S. D. Kulkarni, A. G. Marut, and L. C. Kempel, "Method of moments solution for a printed patch/slot antenna on a thin finite dielectric substrate using the volume integral equation," *IEEE Trans. Antennas Propag.*, vol. 54, no. 4, pp. 1174–1184, Dec. 2007.

[6] J. X. Wan, T. M. Xiang, and C. H. Liang, "The fast multipole algorithm for analysis of large-scale microstrip antenna arrays," *PIER 49, Progr. Electromagn. Res.*, pp. 239–255, 2004.

[7] L. Tsang, C. J. Ong, C. C. Huang, and V. Jandhyala, "Evaluation of the Green's function for the mixed potential integral equation (MPIE) method in the time domain for layered media," *IEEE Trans. Antennas Propag.*, vol. 51, no. 7, pp. 1559–1571, Jul. 2003.

[8] M. E. Yavuz, M. I. Aksun, and G. Dural, "Critical study of the problems in discrete complex image method," in *Proc. IEEE Int. Symp. Electromagn. Compat.*, May 11–16, 2003, vol. 2, pp. 1281–1284.

[9] D. G. Fang, J. J. Yang, and G. Y. Delisle, "Discrete image theory for horizontal electric dipoles in a multilayered medium," *Proc. Inst. Elec. Eng.*, vol. 135, pp. 297–303, 1988, pt. H.
[10] W.-H. Tang and S. D. Gedney, "An efficient application of the discrete complex image method for quasi-3-D microwave circuits in layered media," *IEEE Trans. Microw. Theory Tech.*, vol. 55, no. 8, pp. 1723–1729, Aug. 2007.
[11] J. J. Yang, Y. L. Chow, G. E. Howard, and D. G. Fang, "Complex images of an electric dipole in homogenous and layered dielectrics between two ground planes," *IEEE Trans. Microw. Theory Tech.*, vol. 40, no. 3, pp. 1358–1362, Mar. 1992.
[12] Y. L. Chow, J. J. Yang, and G. E. Howard, "Complex images for electrostatic field computation in multilayered media," *IEEE Trans. Microw. Theory Tech.*, vol. 39, no. 7, pp. 1120–1125, Jul. 1991.
[13] Y. Hua and T. K. Sarkar, "Generalized pencil-of-function method for extracting poles of an EM system from its transient response," *IEEE Trans. Antennas Propag.*, vol. 37, no. 2, pp. 229–234, Feb. 1989.
[14] N. Hojjat, S. Safavi-Naeini, R. Faraji-Dana, and Y. L. Chow, "Fast computation of the nonsymmetrical components of the Green's function for multilayer media using complex images," *Proc. Inst. Elect. Eng. Microw. Antennas Propag.*, vol. 145, no. 4, pp. 285–288, Aug. 1998.
[15] K. A. Michalski and J. R. Mosig, "Multilayered media Green's function in integral equation formulations," *IEEE Trans. Antennas Propag.*, vol. 45, no. 3, pp. 508–519, Mar. 1997.
[16] M. I. Aksun and G. Dural, "Clarification of issues on the closed-form Green's functions in stratified media," *IEEE Trans. Antennas Propag.*, vol. 53, no. 11, pp. 3644–3653, Nov. 2005.
[17] M. Ayatollahi and S. Safavi-Naeini, "A new representation for the Green's function of multilayer media based on plane wave expansion," *IEEE Trans. Antennas Propag.*, vol. 52, no. 6, pp. 1548–1557, Jun. 2004.
[18] B. Hu and W. C. Chew, "Fast inhomogeneous plane wave algorithm for scattering from objects above the multilayered medium," *IEEE Trans. Geosci. Remote Sens.*, vol. 39, pp. 1028–1038, May 2001.
[19] A. Yariv, *Optical Electronics in Modern Communications*, 5th ed. New York: Oxford Univ. Press, 1997.
[20] E. Cavanagh and B. Cook, "Numerical evaluation of Hankel transforms via Gaussian-Laguerre polynomial expansions," *IEEE Trans. Acoust., Speech, Signal Process.*, vol. 27, no. 4, pp. 361–366, Aug. 1979.
[21] M. M. Tajdini and A. A. Shishegar, "The Gaussian expansion of the Green's function of an electric current in a parallel-plate waveguide," in *Proc. IEEE Int. RF Microw. Conf.*, Dec. 2–4, 2008, pp. 223–225.
[22] M. J. Bastiaans, "Gabor's expansion of a signal into Gaussian elementary signals," *Proc. IEEE*, vol. 68, no. 4, pp. 538–539, Apr. 1980.
[23] H.-T. Chou, P. H. Pathak, and R. J. Burkholder, "Novel Gaussian beam method for the rapid analysis of large reflector antennas," *IEEE Trans. Antennas Propag.*, vol. 49, no. 6, pp. 880–893, Jun. 2001.
[24] H.-T. Chou and P. H. Pathak, "Use of Gaussian ray basis functions in ray tracing methods for applications to high frequency wave propagation problems," *Proc. Inst. Elect. Eng. Microw. Antennas Propag.*, vol. 147, no. 2, pp. 77–81, Apr. 2000.
[25] R. E. Collin, *Field Theory of Guided Waves*, 2nd ed. New York: McGraw-Hill, 1991.
[26] Y. L. Chow, J. J. Yang, D. G. Fang, and G. E. Howard, "A closed form spatial Green's function for the thick microstrip substrate," *IEEE Trans. Microw. Theory Tech.*, vol. 39, no. 3, pp. 1358–1362, Mar. 1991.
[27] K. A. Michalski, "Extrapolation methods for Sommerfeld integral tails," *IEEE Trans. Antennas Propag.*, vol. 46, no. 10, pp. 1405–1418, Oct. 1998.
[28] G. B. Arfken and H. J. Weber, *Mathematical Methods for Physicists*, 6th ed. Burlington, MA: Elsevier Academic Press, 2005.
[29] M. I. Aksun, M. E. Yavuz, and G. Dural, "Comments on the problems in DCIM," in *Proc. IEEE APS Int. Symp. USNC/CNC/URSI North Amer. Radio Sci. Meeting Conf.*, Jun. 22–27, 2003, pp. 673–676.
[30] Agilent ADS 2002 Agilent Technologies [Online]. Available: http://www.agilent.com

Mohammad Mahdi Tajdini (S'09) received the B.Sc. and M.Sc. degrees in electrical engineering from the University of Tehran and Sharif University of Technology, Tehran, Iran, in 2006 and 2008, respectively. He is currently working toward the Ph.D. degree at Northeastern University, Boston, MA.

From 2007 to 2009, he was with the Numerical Electromagnetic Laboratory, Sharif University of Technology, as a Graduate Student Researcher. He is currently a Graduate Research Assistant in the Applied EM and Optical Devices Laboratory, Northeastern University. His research interests include theoretical electromagnetics, nanoelectromagnetics, THz communications, physics and applications of metamaterials, and modern physics.

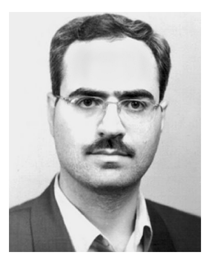

Amir Ahmad Shishegar (M'03) received the B.Sc. (with honors), M.Sc. and Ph.D. degrees in electrical engineering from the University of Tehran, Tehran, Iran.

He was a Visiting Scholar with the University of Waterloo and Apollo Photonics Inc., Canada, during 1999 and 2000. He is currently an Assistant Professor in the Department of Electrical Engineering, Sharif University of Technology. His research interests and activities include analytical and computational electromagnetics, electromagnetic wave propagation modeling, analysis and design of passive optical devices and optical integrated circuits. He held different research and development positions in the field of optical communications, microwave and antennas in a number of private and governmental telecom industries and research organizations including Iran Telecommunication Research Center (ITRC).

Dr. Shishegar is currently the Treasurer of the IEEE-Iran Section.